Impact of elongation on peeling–ballooning stability in TCV H-mode pedestals

O. Sundberg[1], B. Labit[2], L. Frassinetti[1], S. Saarelma[3], A. Mele[2], A. Stagni[4], A. Lafay-Labrosse[1], the TCV team*, and the EUROfusion Tokamak Exploitation team**

[1]*Department of Electromagnetics and Plasma Physics, KTH Royal Institute of Technology, Stockholm, Sweden*

[2]*Ecole Polytechnique Fédérale de Lausanne (EPFL), Swiss Plasma Center (SPC), Lausanne, Switzerland*

[3]*UKAEA Culham, Culham Science Centre, Abingdon, Oxfordshire, OX14 3DB, United Kingdom*

[4]*Consorzio RFX (CNR, ENEA, INFN, Università di Padova, Acciaierie Venete SpA), Padova, Italy*

**See the author list of C. Theiler et al 2026 Nucl. Fusion 66 116007*

***See the author list of N. Vianello et al 2026 Nucl. Fusion 66 116010*

ITER pedestals are expected to be limited by low-n peeling instabilities, partly due to the very low electron-electron pedestal collisionality (${\nu_{ee}^*}^{\text{ped}}$) foreseen for ITER. This has also been found in predictive pedestal modelling over the last decade and a half [1,2,3]. In view of these results, studies of peeling-limited regimes in present-day tokamaks are of great interest for the fusion community. However, existing European tokamaks operate predominantly in a ballooning-limited regime, with pedestals limited by high-n ballooning instabilities.

Efforts have therefore been made to access peeling-limited pedestals in European tokamaks, with successful experiments in JET, MAST-U, and TCV [3,4]. In TCV, however, previous peeling-limited pedestals were found close to the nose of the peeling-ballooning stability boundary, rather than deeply in the low-n peeling branch [3].

Modelling studies in KSTAR [5] and experimental results in MAST-U [4] have shown that plasma elongation (κ) has a strong impact on pedestal stability. In particular, increasing κ stabilizes high-n ballooning modes and shifts the dominant instability toward lower-n modes. In $j - \alpha$ space, where j is the normalized pedestal current density and α is the normalized pressure gradient, this corresponds to a shift of the stability boundary toward higher α, associated with the stabilization of the ballooning branch. These results suggest that increasing κ may provide a route to access more strongly peeling-limited pedestals in TCV.

Table 1. *Shot number, time interval, and average κ for the analysed profiles.*

Shot	Time interval [s]	$\langle\kappa\rangle$
#81545	$0.80 - 0.95$	1.71
#81545	$1.10 - 1.23$	1.84
#81586	$1.28 - 1.32$	2.01

To test this hypothesis, a set of high-κ H-mode experiments conducted in TCV was analysed. Two discharges were selected: #81545 and #81586, with the time intervals and average κ listed in Table 1. The discharges were heated purely via $\sim$ 1.8MW X3 ECRH and both were operated at 430kA/1.43T, with only small variations in total normalized pressure, $\beta_N \approx$ 1.48-1.65, across the κ scan dataset.

Figure 1 summarizes the main characteristics of the dataset. Figure 1(a) compares the elongation and pedestal collisionality achieved in the κ scan dataset with earlier high-${\nu_{ee}^*}^{\text{ped}}$ ballooning-limited pedestals and low-${\nu_{ee}^*}^{\text{ped}}$ peeling-limited pedestals from [6]. The new dataset reaches ${\nu_{ee}^*}^{\text{ped}} \sim 0.3$, which is lower than the earlier TCV ballooning-limited dataset and more comparable to the earlier peeling-limited dataset [6]. The κ scan pedestals are characterized by $n_e^{\text{ped}} \approx 4.0\text{-}4.5 \times 10^{19}$ m^{-3} and $T_e^{\text{ped}} \approx 0.50\text{-}0.55$ keV, with n_e^{ped} comparable to the earlier ballooning-limited dataset and T_e^{ped} closer to the earlier peeling-limited dataset. The relatively low ${\nu_{ee}^*}^{\text{ped}}$ is also partially due to a lower q_{95}, which is roughly a factor of two lower than the earlier datasets (due to the higher plasma current). This new κ scan dataset extends the available TCV database toward higher κ.

The plasma boundaries in Figure 1(b) show that the scan is obtained mainly by increasing the upper elongation. Within the scatter of the data, the electron pressure profiles in Figure 1(c) show no large variations in pedestal height, width, or gradient across the κ scan. The measurements are extracted from pre-ELM Thomson scattering data in the time intervals listed in Table 1. However, for the highest κ the available time interval is very short, making the extracted profiles less robust than for the other κ values.

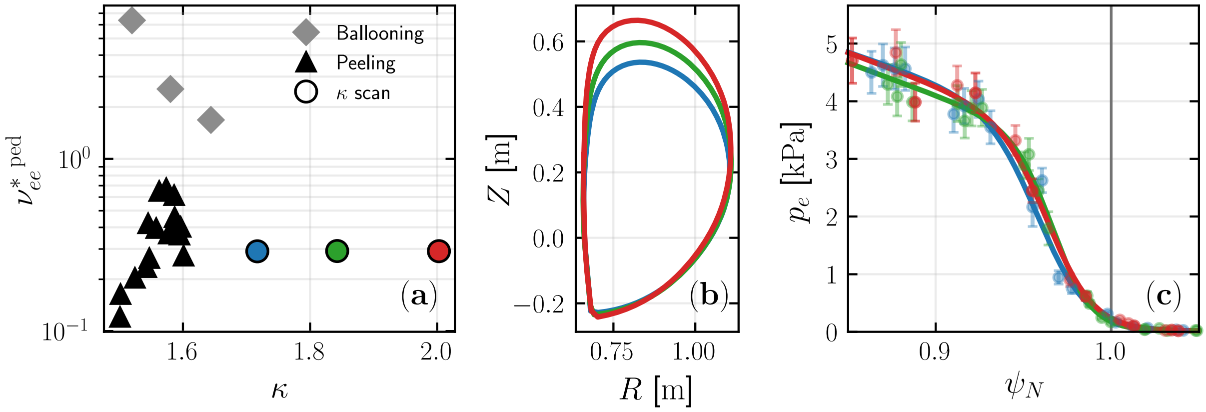

Figure 1. *Dataset overview. (a) $\nu_{ee}^{*\,ped}$ as a function of κ for earlier TCV ballooning- and peeling-limited datasets [6], together with the new κ scan dataset. (b) Experimental plasma boundaries for the κ scan. (c) Experimental p_e profiles for the three analysed time windows. Thomson scattering measurements are shown by circles and* mtanh *fits by solid lines.*

The following assumptions were used in the analysis. Due to the high vertical plasma position, no CXRS measurements were available, and $T_i = T_e$ was assumed. A separatrix electron temperature $T_e^{sep} = 81$ eV, calculated for the $\kappa = 1.84$ case using the two-point model implemented in [7], was used for all cases. Sensitivity scans with a $\pm 20\%$ variation of T_e^{sep} did not change the conclusions for the other κ values. Furthermore, $Z_{\text{eff}} = 2.4$ and $q_0 \sim 1$ were used throughout the analysis.

The peeling-ballooning stability was calculated using a HELENA-MISHKA workflow, with HELENA being a fixed boundary equilibrium code and MISHKA being a linear ideal MHD stability code [1,8,9]. Figure 2(a) shows the results using the diamagnetic criterion ($\gamma/\omega_{\max}^* > 0.25$), while Figure 2(b) shows the results using the Alfvén criterion ($\gamma/\omega_{\text{A}} > 0.03$). In both cases, increasing κ shifts the stability boundary toward higher α, resulting in higher experimental normalized pressure gradients, α_{exp}, even though the pressure profiles remain similar, as shown in Figure 1(c). This can partly be attributed to the normalization of α, which depends on the plasma volume $V(\psi)$, meaning that changes in plasma shape can affect α even for similar pressure profiles, as also noted in [4]. Furthermore, a reduction in the toroidal mode number of the most unstable mode, n_{crit}, is observed for increasing κ.

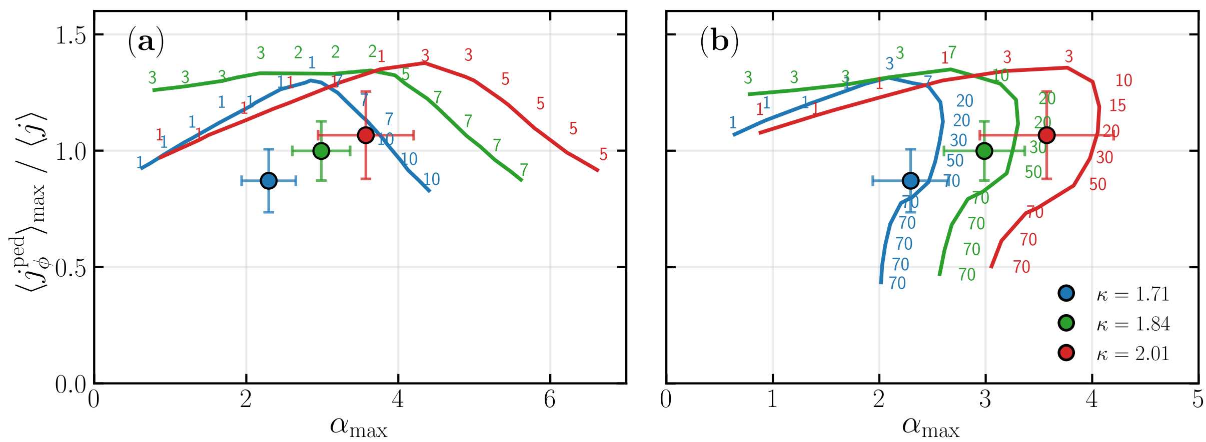

Figure 2. *Peeling-ballooning stability for the three κ values in the κ scan dataset. Results are shown for both (a) the diamagnetic criterion and (b) the Alfvén criterion. The stability boundaries are shown by solid lines, the operational points by circles, and the most unstable n by the numbers.*

The observed shift in the stability boundary is consistent with previous MAST-U and KSTAR studies [4,5]. Increasing κ stabilizes the ballooning instabilities, shifting the limiting modes toward lower n. With the Alfvén criterion, n_{crit} decreases from approximately $n =$ 50-70 at $\kappa = 1.71$ to $n =$ 15-30 at $\kappa = 2.01$. With the diamagnetic criterion, the $\kappa = 2.01$ pedestal appears to operate deeper in the low-n peeling branch than previously reported in TCV [3], being limited by $n = 1$ modes. These results suggest that increasing κ at low collisionality can move TCV pedestals closer to a peeling-limited regime.

The predictive pedestal code Europed [10], based on the EPED model [11], was used to assess whether the experimental trends could be reproduced in simulations. Since the Alfvén criterion places the experimental pedestals closer to marginal stability, the Europed analysis below focuses on this criterion for simplicity. The $\kappa = 1.84$ case was used as the reference, with the experimental n_e^{ped}, n_e^{sep}, and β_N as inputs. Europed implements the standard relation: $w = c_{\mathrm{KBM}}\sqrt{\beta_\theta^{\mathrm{ped}}}$, where w is the pressure pedestal width and $\beta_\theta^{\mathrm{ped}}$ is the poloidal beta at the pedestal top. The KBM width constant c_{KBM} was calibrated to reproduce the experimental profiles, giving good agreement for $c_{\mathrm{KBM}} = 0.11$. The plasma boundary was then changed to the lower- and higher-κ cases, while keeping other parameters such as β_N, I_P, and B_T fixed.

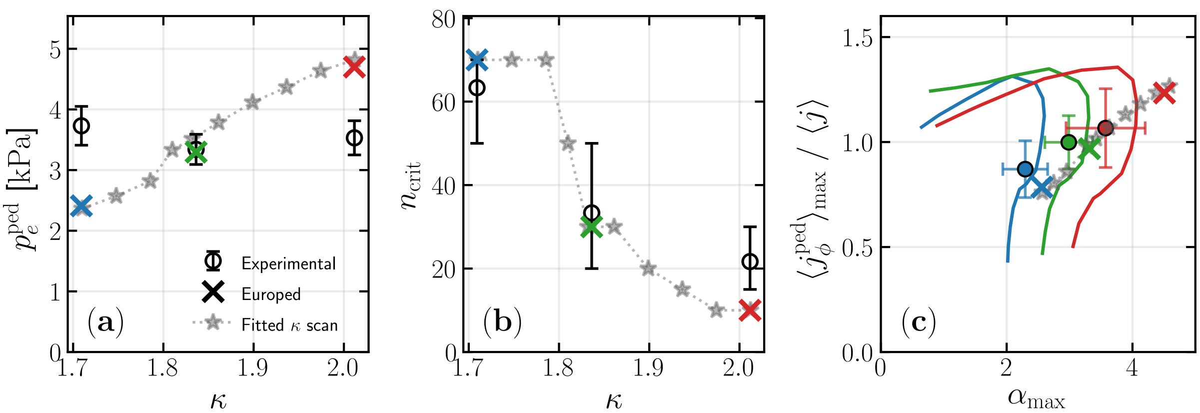

***Figure 3**. Europed predictions with $c_{KBM} = 0.11$. (a) p_e^{ped}, defined from the mtanh fit, as a function of κ. (b) n_{crit} as a function of κ. (c) Experimental peeling-ballooning stability together with Europed predictions. Crosses show Europed predictions using the experimental boundaries, while stars show the fitted κ scan.*

The results obtained by changing only the experimental boundary at $c_{\mathrm{KBM}} = 0.11$ are shown by crosses in Figure 3. The reference $\kappa = 1.84$ case is well reproduced by construction. However, Figure 3(a) shows that the pedestal height is underestimated for $\kappa =$ 1.71 and overestimated for $\kappa = 2.01$. Despite this lack of quantitative agreement in p_e^{ped}, Europed reproduces the decrease in n_{crit} with increasing κ, as shown in Figure 3(b). Figure 3(c) shows that Europed qualitatively captures the elongation dependence of the peeling-ballooning stability, with the predicted α_{crit} increasing with κ. For $\kappa = 1.71$ and $\kappa = 1.84$, the predictions are within the experimental uncertainty, while α_{crit} is overpredicted for $\kappa =$ 2.01. This may be related to the experimental pedestal being further from marginal stability for the highest $\kappa = 2.01$ case.

To isolate the effect of elongation and assess the trends more accurately, a finer κ scan was performed in Europed. The $\kappa = 1.84$ boundary was fitted using the Luce parametrization introduced in [12], after which the upper elongation was varied within the experimental range. The resulting scan, shown by stars in Figure 3, is consistent with the Europed predictions based on the experimental boundaries. This indicates that the dominant effect is associated

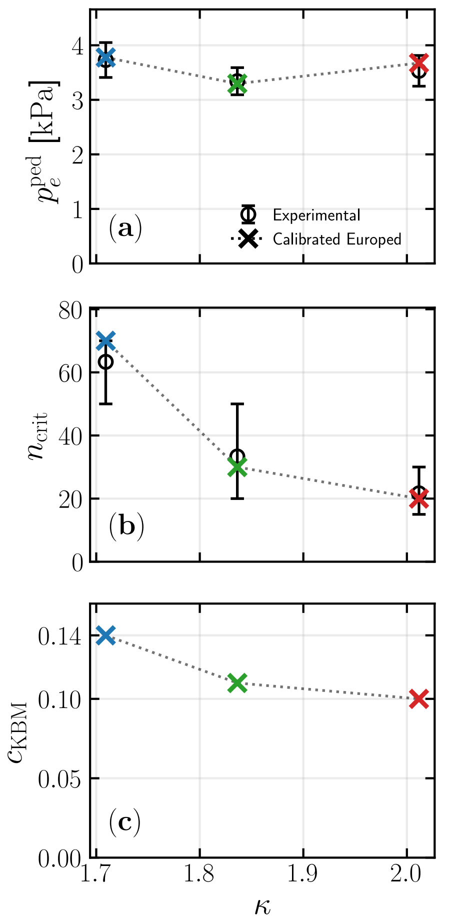

Figure 4. *Individually calibrated Europed predictions: (a) p_e^{ped}, (b) n_{crit}, and (c) calibrated c_{KBM}, all as a function of κ.*

with κ, rather than with other shape parameters that vary slightly during the experimental κ scan, such as squareness.

Finally, ad-hoc Europed calibrations were performed separately for each κ to investigate why using a fixed $c_{\mathrm{KBM}} = 0.11$ does not reproduce the experimental profiles across the κ scan. The experimental n_e^{ped}, n_e^{sep}, and β_N were used for each κ, while c_{KBM} was varied to reproduce the experimental profiles. The results are shown in Figure 4. With individual calibration, p_e^{ped} is reproduced accurately for all κ values, as seen in Figure 4(a). The width and the gradient agreement were also reasonable, although weaker for $\kappa = 2.01$. Figure 4(b) shows that the decrease in n_{crit} with increasing κ is still reproduced.

As shown in Figure 4(c), the calibrated c_{KBM} decreases with increasing κ; from $c_{\mathrm{KBM}} = 0.14$ at $\kappa = 1.71$ to $c_{\mathrm{KBM}} = 0.10$ at $\kappa = 2.01$. The variations in n_e^{ped}, n_e^{sep}, and β_N had only a small impact, indicating that most of the improvement comes from the change in c_{KBM}. This suggests a possible shape dependence of the KBM width constant, which may indicate that the pedestal turbulent transport changes with elongation. However, confirming this interpretation would require gyrokinetic transport analysis and dedicated experimental edge turbulence measurements.

In conclusion, this study shows that the effect of elongation on peeling-ballooning stability in TCV is consistent with previous results from KSTAR and MAST-U [5,4]. Increasing plasma elongation increases α and decreases n_{crit}, shifting the pedestal stability toward a more peeling-limited regime. Europed captures the elongation dependence of the stability reasonably well. However, quantitative agreement with the experimental profiles across the full κ scan is not obtained with $c_{\mathrm{KBM}} = 0.11$. Individual calibration suggests that c_{KBM} decreases with increasing κ, indicating that a shape-dependent c_{KBM} may be required.

To strengthen these conclusions, further dedicated high-κ H-mode experiments are needed, preferably with stationary high elongation and longer ELMy phases. Such experiments would reduce the uncertainty in the results and enable measurements of edge turbulent transport, which together with gyrokinetic analysis could assess how elongation affects pedestal transport. Finally, ion temperature measurements would allow the $T_i = T_e$ assumption to be tested directly.

This research is supported by Vetenskapsrådet, under Grant Numbers 2023-04895 and by Energimyndigheten under the contract number 2023-204940. This work has been carried out within the framework of the EUROfusion Consortium, partially funded by the European Union via the Euratom Research and Training Programme (Grant Agreement No 101052200 — EUROfusion). The Swiss contribution to this work has been funded by the Swiss State Secretariat for Education, Research and Innovation (SERI). Views and opinions expressed are however those of the author(s) only and do not necessarily reflect those of the European Union, the European Commission or SERI. Neither the European Union nor the European Commission nor SERI can be held responsible for them.

REFERENCES

[1] Saarelma et al, NF, 2012
[2] Snyder et al, NF, 2011
[3] Frassinetti et al, NF, 2026
[4] Imada et al, NF, 2024
[5] Kim et al, PoP, 2022
[6] Frassinetti et al, EPS 2022
[7] Stangeby et al, NF, 2015
[8] Huysmans et al, IJoMP C, 1991
[9] Mikhailovskii et al, PPR, 1997
[10] Saarelma et al, PPCF, 2018
[11] Snyder et al, PoP, 2009
[12] Luce et al, PPCF, 2013